30 years in the life of an active submarine volcano: A time-lapse bathymetry study of the Kick-'em-Jenny Volcano, Lesser Antilles

R. W. Allen[1], C. Berry[1], T. J. Henstock[2], J. S. Collier[1], F. J-Y. Dondin[3], A. Rietbrock[4], J. L. Latchman[3], R. E. A. Robertson[3]

[1]Department of Earth Science and Engineering, Imperial College London, SW7 2AZ
[2]Ocean and Earth Science, National Oceanography Centre Southampton, SO14 3ZH
[3]The UWI Seismic Research Centre, St Augustine, Trinidad and Tobago
[4]School of Environmental Sciences, University of Liverpool, L69 3GP

Corresponding Author: Robert Allen (r.allen16@imperial.ac.uk)

Key Points:

- New and reprocessed bathymetric datasets document depth changes at the Kick-'em-Jenny volcano over a period of 32 years.
- Comparison with other recent studies of submarine arc volcanoes identifies clear similarities in the styles of depth changes observed.
- We confirm the value of repeat swath bathymetry surveys for assessing potential submarine volcanic hazards.

Abstract

Effective monitoring is an essential part of identifying and mitigating volcanic hazards. In the submarine environment this is more difficult than onshore because observations are typically limited to land-based seismic networks and infrequent shipboard surveys. Since the first recorded eruption in 1939, the Kick-'em-Jenny (KeJ) volcano, located 8km off northern Grenada, has been the source of 13 episodes of T-phase signals. These distinctive seismic signals, often coincident with heightened body-wave seismicity, are interpreted as extrusive eruptions. They have occurred with a recurrence interval of around a decade, yet direct confirmation of volcanism has been rare. By conducting new bathymetric surveys in 2016 and 2017 and reprocessing 4 legacy datasets spanning 30 years we present a clearer picture of the development of KeJ through time. Processed grids with a cell size of 5m and vertical precision on the order of 1-4m allow us to correlate T-phase episodes with morphological changes at the volcano's edifice. In the time-period of observation 7.09×10^6 m^3 of material has been added through constructive volcanism – yet 5 times this amount has been lost through landslides. Limited recent magma production suggests that KeJ may be susceptible to larger eruptions with longer repeat times than have occurred during the study interval, behavior more similar to sub-aerial volcanism in the arc than previously thought. T-phase signals at KeJ have a varied origin and are unlikely to be solely the result of extrusive submarine eruptions. Our results confirm the value of repeat swath bathymetry surveys in assessing submarine volcanic hazards.

1 Introduction

Accurately quantifying the risk associated with volcanic hazards requires detailed monitoring and where possible a thorough understanding of the scale and impact of historic events. Technological improvements have made it possible to monitor terrestrial volcanoes to increasingly high degrees of accuracy. Geodetic measurements such as GPS (Parks et al., 2012; Puglisi & Bonforte, 2004; Puglisi et al., 2001), tilt meters (Bonaccorso et al., 2002; Fiske & Shepherd, 1990; Ricco et al., 2013), strain meters (Bonaccorso et al., 2012; Voight et al., 2010) and electronic distance meters (Jackson et al., 1998) create a detailed record of morphological changes through time. When combined with satellite imaging technologies such as Synthetic Aperture Radar (SAR), which has the capacity to measure deformation to centimetre scale accuracy (Massonnet et al., 1995; Massonnet & Feigl, 1998; Parks et al., 2012), and other monitoring techniques including volcanic gas emission (Duffell et al., 2003; Edmonds et al., 2003), seismicity (Aki & Ferrazzini, 2000; Brenguier et al., 2008; Chiarabba et al., 2000), magnetics (Del Negro et al., 2004; Del Negro et al., 2002), microgravity (Budetta et al., 1999; Rymer, 1994), and photogrammetry (Baldi et al., 2000; Diefenbach et al., 2012), these datasets are powerful resources in attempts to assess volcanic risk (Cashman & Sparks, 2013; Dzurisin, 2003; Sparks, 2003).

In the submarine realm the work of monitoring volcanoes is made much more difficult. Events at NW Rota-1 in the Marianna arc (Embley et al., 2006) and West Mata in the NE Lau Basin (Resing et al., 2011) are the only direct visual observations of deep-sea submarine eruptions. Shallow water island-forming eruptions, such as the creation of Surtsey (near Iceland) between 1963-67 (Moore, 1985), Myojinsho between 1952-53 (Fiske et al., 1998) and Nishinoshima (both Japan) between 2013-15 (Maeno et al., 2016), are not uncommon. Yet until fairly recently we had exceedingly limited understanding of the behaviour of deeper submarine volcanoes throughout the eruption cycle despite associated hazards including potentially tsunamigenic landslides and eruptions.

Many more submarine eruptions, both from seamounts and ocean ridges, are now being

recorded and surveyed both before and after volcanic activity (Rubin et al., 2012). Although shipboard surveys are unable to match modern satellite techniques for precision or repeat interval, recent time-lapse bathymetry studies from volcanoes such as Monowai (Chadwick et al., 2008b; Watts et al., 2012; Wright et al., 2008), Santorini (Watts et al., 2015), NW Rota-1 (Chadwick et al., 2012; Schnur et al., 2017) and West Mata (Clague et al., 2011; Embley et al., 2014) have greatly improved our understanding of the evolution of submarine volcanoes. On both Monowai and NW Rota-1 the authors were able to identify multiple episodes of both positive and negative depth changes in the form of landslides tied to volcanic and seismic activity. However, despite their obvious value studies of this nature over submarine volcanoes are still uncommon. Although new technologies for remote sensing of submarine eruptions are emerging e.g. the 2014 instillation of a permanent cabled underwater observatory monitoring Axial Seamount on the Juan de Fuca ridge (Kelley et al., 2014), these methods are still a long way from matching the amount of detailed information which can be gathered during terrestrial volcanic eruptions.

Today, remote detection of submarine eruptions is largely reliant on identifying T-phase arrivals on regional hydrophones and seismometers e.g. Dziak and Fox (1999), Bohnenstiehl et al. (2013). These distinctive hydro-acoustic signals can be produced by submarine earthquakes or by the interaction between water and fresh magma and are capable of travelling long distances through the minimum velocity SOFAR (Sound Fixing and Ranging) channel (Ito et al., 2012; Lindsay et al., 2005; Metz et al., 2016). At KeJ volcanic T-phase arrivals (which are thought to indicate submarine eruptions) are differentiated from signals with a purely seismic origin by their low frequency content, impulsive onset and duration (often several 10s of seconds), regularly running together into a sustained tremor-like signal during periods of high activity (Lindsay et al., 2005). They are also lacking associated P and S wave arrivals as would be expected from a signal with an earthquake source.

In this paper we present new and reprocessed multibeam bathymetry data covering a period of more than 30 years over the volcano Kick-‘em-Jenny (KeJ) in the southern Lesser Antilles. New bathymetric surveys conducted from the R.R.S. James Cook in 2016 and 2017 combined with legacy datasets from 1985, 2003, 2013 and 2014 allow us to view morphological changes at the volcano through to the present day. The surveys span several episodes of recorded volcanic T-phases in 1988, 1995, 2001 (Lindsay et al., 2005), 2015 (Robertson et al., 2015) and 2017 (Latchman et al., 2017). By combining these datasets we are able to describe the changes to the edifice through time and offer insight into the processes controlling the evolution of submarine volcanoes.

2 Kick-‘em-Jenny

2.1 Eruption History and Hazard

KeJ sits near the southern end of the Lesser Antilles island arc with a current summit depth of 197m b.s.l.. Located 8km north of the island of Grenada it is the only known active submarine volcano in the region (Figure 1). The arc, active since the Cretaceous (Bouysse, 1988; Bouysse & Westercamp, 1990), is located above the site where Atlantic oceanic crust is slowly subducting beneath the Caribbean plate at rates of ~2cm/yr (Symithe et al., 2015). Of the arc’s terrestrial volcanoes Soufrière Hills on Montserrat has seen the most activity in recent years having been in a constant state of eruption since 1995 (Druitt & Kokelaar, 2002; Wadge et al., 2014).

KeJ lavas are commonly olivine basalts and basaltic andesites (Devine & Sigurdsson, 1995;

Sigurdsson & Shepherd, 1974). Similar compositions are common throughout Grenada and much of the southern Grenadines (Sigurdsson & Shepherd, 1974). It has been proposed that KeJ is the active vent of a larger volcanic system (Lindsay et al., 2005) which also encompasses nearby islands such as Isle de Ronde and Isle de Caille (Figure 1). There is evidence for both explosive and effusive eruptions at KeJ, though the former seems to be by far the more common. ROV observations have documented extensive explosive breccias and pyroclastic deposits (Carey et al., 2016; McClelland et al., 1989), but little to no evidence of lava flows (Sigurdsson & Shepherd, 1974), though there was an episode of dome building tied to volcanic activity in 1977 (Devine & Sigurdsson, 1995).

KeJ was unknown until 1939, when a large eruption occurred which was observed from northern Grenada. Local reports describe an ash cloud extending ~300m above sea level and ground shaking in the north of the island (Devas, 1974). Since then there have been 13 notable episodes of T-phase signals attributed to KeJ (Figure 2) interpreted as submarine eruptions (Lindsay et al., 2005), the most recent of these occurred in April 2017 (Latchman et al., 2017). T-phases have been recorded in association with KeJ as far back as 1943 despite the presence of only a couple of seismometers in the Caribbean at this time (Lindsay et al., 2005). Repeat times between periods of activity, on the order of a decade, mean that KeJ is considered one of the Antilles arc's most active volcanoes. Based purely on visual observations the 1939 eruption was by far the largest, with only two further events (1974 and 1988) showing low-level signs of activity at the sea surface, limited to water discolouration and small volumes of ejecta (Bouysse et al., 1988; Lindsay et al., 2005; McClelland et al., 1989).

In 2001, 2015 and 2017 T-phase activity was preceded by several days of heightened seismicity around the volcano (Latchman et al., 2017; Lindsay et al., 2005; Robertson et al., 2015). However, reports of shaking from northern Grenada (and on occasion as far away as Martinique) coincide with the majority of instrumental T-phase recordings (Latchman et al., 2017; Lindsay et al., 2005; McClelland et al., 1988; Robertson et al., 2015; Shepherd & Robson, 1967), so this correlation with seismic activity is not an entirely new phenomenon.

A near-shore location and history of regular activity means that KeJ is a major concern for inhabitants of the southern Caribbean islands. The shallow water and complex topography between the islands makes the specifics of any tsunami in this region hard to model (Harbitz et al., 2012; Smith & Shepherd, 1996) though due to the volume of material required, the risk of a tsunami triggered by eruption alone, and without some additional major mass-movement is considered minimal (Gisler et al., 2006). Recent modelling of such an event has shown that a collapse at the edifice in the region of $0.7km^3$ could trigger large enough waves to cause hazardous run-up on local islands (Dondin et al., 2017). Lindsay et al. (2005) concluded that the risk posed to shipping by gas release and ejecta during eruptions was the more pressing and likely hazard concern posed by KeJ. Such gas releases are possible outside of periods of volcanic activity.

2.2 Morphology

The perceived risk associated with KeJ has motivated 15 bathymetric surveys starting with the H.M.S. Vidal in 1962 (Figure 2). This wealth of data means that the general morphology of KeJ is well known. The volcano consists of an asymmetric circular cone with a central crater measuring approximately 300m in diameter. The peak height of the rim, (currently at ~197m b.s.l.), has remained fairly constant through time, besides a period of dome building in the 1970s/80s when it was observed as shallow as 160m (Figure 2). Recent measurements have disproved the previously erroneous view that KeJ was growing rapidly towards the surface and

has the potential to form a new volcanic island (Devine & Sigurdsson, 1995; Watlington et al., 2002). Such conclusions were largely driven by an error in the depth measurement made from the H.M.S. Vidal (1962) which put the summit at 232m b.s.l. (Lindsay et al., 2005). The current edifice is situated on the flanks of the Lesser Antilles arc ridge and stands 1300m above the Grenada back-arc Basin to the west.

The cone sits within a large collapse scarp (Figure 3). This horseshoe shaped feature, up to 14km long and 6km wide is the result of a near-total collapse of a previous incarnation of KeJ. This "proto-Jenny" is modelled to have stood significantly above sea-level before failure at approximately 43ka (Dondin et al., 2012; Dondin et al., 2017). Evidence for similar high volume sector collapses and slope failures are observed at almost all of the major island volcanoes along the arc (Boudon et al., 2007; Deplus et al., 2001; Watt et al., 2012a; Watt et al., 2012b). Globally such events, as well as submarine volcanic explosions, are frequently tsunamigenic (Paris et al., 2014). The debris flow created by the collapse of proto-Jenny is clearly observable on bathymetry for over 14km onto the plain of the Grenada Basin with an approximate volume of 4.4km^3 (Carey et al., 2014; Dondin et al., 2012). The modern cone of KeJ has grown through this older debris flow. A major failure on this scale today would certainly be capable of triggering a regional tsunami. However, given the smaller size of the cone (a total volume of 0.585km^3 measuring down to the 600m contour), and greater depth below sea level it is unlikely that a major sector collapse at KeJ today would have such a significant impact.

KeJ is a highly active hydrothermal system, with numerous surveys and ROV studies observing active venting both from within the crater (Carey et al., 2016; Graff et al., 2008; Koschinsky et al., 2007; Wishner et al., 2005) and on the flanks of the edifice (Koschinsky et al., 2007). Emanating fluid temperatures have reached as high as 270-280°C (Graff et al., 2008; Koschinsky et al., 2007) with volcanic sediment within the crater showing evidence for extensive alteration to clay minerals and surface Fe-oxyhydroxide mineralisation (Carey et al., 2016). These harsh conditions, coupled with the regularity of eruptions and gas releases greatly limits macrofaunal activity within the crater (Graff et al., 2008; Wishner et al., 2005).

The heavily faulted back-wall of KeJ hosts a number of smaller volcanic cones, the largest of these, Kick-'em-Jack, sits shallower than KeJ with a peak depth of 112m b.s.l.. No volcanic activity has been definitively tied to these cones during modern observations of KeJ. In contrast to KeJ, ROV images taken by the R/V Nautilus in 2013/2014 show the edifice of Kick-'em-Jack is home to an array of sub-sea life, and extensive mineralisation is further evidence for a cone which has been dormant in recent time.

3 Data

Data from 6 swath bathymetry surveys are used for this investigation (Figure 2). These surveys from the R/V Robert D. Conrad (1985), R/V Ronald M. Brown (2003), R/V Nautilus (2013 & 2014) and R.R.S. James Cook (2016 & 2017) cover a period of 32 years and 5 seismic episodes (1988, 1990, 2001, 2015 and 2017) at KeJ. The acquisition parameters of each of the surveys can be found in Table 1. The survey geometries and further data quality information (grid standard deviation and sounding density) are also shown in two additional figures in the supplementary materials.

The R.R.S. James Cook surveys recorded the bathymetry on both EM710 (~70-100Hz - high frequency system designed for use in shallow water) and an EM120 (12Hz – low frequency deep water system) multibeam echo sounder, with the EM120 covering a much larger spatial

extent down-dip to the west of KeJ. In this down-dip region geologically significant differences between the surveys were minimal (Berry, 2017). From here on, discussion of the R.R.S. James Cook surveys will refer to the higher resolution survey done across the edifice of KeJ with the EM710 system. We reprocessed both the 2013 and 2014 Nautilus surveys, but there are no significant morphological changes between them (Berry, 2017). The 2013 survey was of significantly higher quality and so we will not present the 2014 data in the following analysis. Backscatter data was also reviewed for the two R.R.S. James Cook surveys, however the results of these were inconclusive and so will not be shown here.

The surveys from the Brown, Nautilus and Cook were received as raw, unedited swath bathymetry files (xyz format for the Brown dataset and gsf format for the Nautilus datasets) which were processed in the bathymetry editing programme CARIS/HIPS to remove noisy data such as during ROV operations and erroneous depth soundings, particularly from the outer beams. The decision to reprocess this data was taken in order to ensure consistency in editing over all surveys, increasing confidence in our final interpretations. All work was conducted in UTM zone 20N.

Final depth surfaces were gridded at a horizontal resolution of 5m (Figure 4). The edited data from the R.R.S. James Cook and R/V Nautilus were gridded using the CARIS/HIPS Uncertainty Weight algorithm which was found to produce grids with the lowest standard deviation within each cell (Table 1). In this algorithm the contribution of an individual sounding is scaled according to its depth uncertainty (this depth uncertainty takes into account both the distance from the node and the sounding's horizontal uncertainty). It was not possible to run this algorithm on the older R/V Ronald H. Brown data, and so a Swath Angle Weight algorithm was used in which the inner beams are weighted more highly due to their higher incidence angle to the seabed.

When tested on the newer data sets it was found that the Swath Angle algorithm generally added between 1-2m to the standard deviation of the cells in the final grid compared to the Uncertainty Weight algorithm. This in part explains the comparatively high mean deviation of 7.8m for the 2003 grid. In the case of the final 2013 R/V Nautilus grid, the mean standard deviation of depth soundings contributing to each grid cell is just 1.1m (Table 1). The high precision is likely the result of a relatively oversampled grid (Table 1). The 30Hz EM302 instrument used for the survey is also less susceptible to noise than the high frequency system used on the R.R.S. James Cook. Any small gaps in the data were removed by interpolating values based on an area of 5x5 cells around any missing grid squares. Such gaps were largely down-dip from the area of interest around the edifice, and these interpolated values have little impact on our final results (see Figure S1, supplementary materials).

Raw swath files were unavailable for the 1985 dataset which was sourced from the NOAA (National Oceanic and Atmospheric Administration) archive as edited swaths in mbsystem format. The data was not further edited by us but simply extracted as xyz values and gridded in GMT using a continuous curvature surface algorithm with a tension of 0.35 (recommended for steep topography). Due to the significantly lower sounding density of this data set (Table 1, also see additional figures in supplementary materials) a cell size of 30m was used.

Prior to calculation of the depth changes between the multibeam surveys, mean depths were calculated for each grid over a presumed stable area of ~10km^2 down dip to the west of the volcano. There is no evidence for long wavelength inflation or deflation of the study area during the survey interval. Final grids were shifted in depth so as to match the R/V Nautilus

(2013) survey, the most precise dataset used in the study (Table 1). A similar process was used by Wright et al. (2008) in their study of Monowai. Surveys were processed with the same water column velocity model which had been applied by the collecting organisation. Water column velocity measurements made during the surveys by the R.R.S. James Cook reduce from 1540ms^{-1} at the surface to 1490ms^{-1} at 600m depth. At such depths you would only need a mean water column velocity error of around 12ms^{-1} to cause a 5m depth change. The largest mean-depth offset observed from the other surveys to the Nautilus grid was ~2m (see Table 1) an entirely reasonable amount of error considering the difference in the age and design of the bathymetric systems, and potential errors arising from sea-state. No tidal correction was made during processing due to the very low tidal range in the waters around Grenada (maximum ~0.5m).

Positioning errors were always expected to be minimal and none of the calculated depth change grids show strong or consistent errors resulting from offsets in topography. As an example the R.R.S. James Cook uses an Applanix POS MV 320 Global Positioning System (GPS) which is expected to be accurate to 0.5-2m. Any errors on this scale will not be visible once the data are gridded at 5m. This is of greater concern for the older surveys, particularly the 1985 R/V Robert D. Conrad bathymetry, given its age. However the difference images show none of the artefacts expected from positioning errors so we are confident that the positioning is consistent.

Depth change grids were calculated in ArcGIS (Figure 5) by subtracting time-adjacent surveys. To reduce noise, subtractions were clipped at a base value thus retaining only the most significant morphological changes and making them easier to interpret. A value of 5m was chosen for the most recent time-lapses, while 30m was used for the 1985-2003 grid, which is heavily influenced by the comparatively low data density of the Conrad survey (Table 1, also see additional figures in supplementary materials). These values were chosen as they are close to the standard deviation of the difference grids themselves. Changes in volume resulting from the most significant of these depth changes were then calculated from the cleaned difference grids and are shown in table 2.

4 Results

The final bathymetric grids show clear variations in the topography of KeJ through time. In all 4 time-lapses we are able to record both positive (growth) and negative (collapse) features. The most significant of these clearly correlate with episodes of T-phase signals.

4.1 1985-2003

The 1985-2003 time-lapse is the longest timespan covered in our study. This 18 year period covers 3 T-phase episodes in 1988, 1990 and 2001.

The 1985 survey shows a number of morphological features that do not appear in the later surveys. In 1985 a small (30m) volcanic dome existed on the northern flank of the crater. Growth of this dome has been tied to the 1977 T-phase episode (the first of the two events post 1939 large enough to be observable from the sea surface), having first been detected in a 1978 bathymetric survey from the R/V Endeavour (Lindsay et al., 2005; Watlington et al., 2002). To the SW of the crater rim is a steep sided volcanic spine. During the period to 2003 both of these structures collapsed (see Figures 5 and 6). The northern dome leaves a deep breach in the crater rim following the removal of 4.62×10^6 m^3 of material, a deepening of up to 70m. This collapse has been tied to the 1988 eruption of KeJ by submersible observations made from the R/V Seward Johnson in 1989 (McClelland et al., 1989; Watlington et al., 2002). The collapse of the spine on the SW flank is the largest morphological change observed in any of our time-lapses

with a loss of 2.18×10^7 m^3 of material and a depth increase of up to 174m.

During the 1985-03 period there is also an 86m rise in the southern rim of the crater. This added a total volume of 4.26×10^6 m^3 to the edifice of KeJ, the largest constructive event observed in any of our time-lapses (Table 2). The overlap between this depth increase and the northern cone collapse means that there was likely some over-printing of the depth changes associated with each event resulting in under-estimation of the volumes of both. Watlington et al.'s (2002) published grid of KeJ, collected by the R/V Malcolm Baldridge in 1996, allows us to tie both this eruption and the collapse on the SW flank to either the 1988 or 1990 T-phase signals. The 1996 grid is morphologically similar to that collected in 2003, with the dome absent, the volcanic spine largely reduced and a reinforced southern rim.

The 1988 episode is the second of the two T-phase events (post 1939) which was observed at the sea surface and is therefore the most likely candidate for the growth of the SE rim of the crater. The destabilising effect of this relatively large eruption could well be the trigger for the two collapses. However, trying to separate out the timeline of changes associated with the three events in this time-lapse is made difficult by the lack of high quality bathymetry during the intervening periods.

2001 was the first T-phase episode at KeJ to be associated with several days of sustained seismic activity (Lindsay et al., 2005). We assume that the majority of this seismicity was related to the movement of magma at depth. Latchman et al. (2017), tie precursory VT signals (volcano-tectonic seismic events) to ascending magma opening a new channel (or widening an existing one), suggesting a less open conduit than pre-2001 eruptions. However Lindsay et al.'s (2005) relocation of these earthquakes places them several km to the north/north-west of the cone of KeJ.

4.2 2003-2013

The 2003-2013 time-lapse covers an extended period of quiescence from 2001 to 2015 (Figure 2), the longest stretch of time without any recorded activity since monitoring of KeJ began. The absence of recorded T-phases coincides with a period in which morphological changes are on a smaller scale than is observed in the other comparisons (Table 2). The only noteworthy change is a small volume of apparent mass wasting from the SW flank of the cone. This area, the location of the volcanic spine collapse in the previous time-lapse, apparently continued to shed material (Figure 5). Given that no T-phases were recorded, this is likely to be a long-term process of erosion of unstable material left behind by the previous collapses rather than an eruption driven collapse. The relatively small volume of -1.88×10^6 m^3 is lost in this way, with a mean depth change of 7.2m.

The NW flank of the cone and much of the crater rim appear to show a weak positive swell during this time period of up to 14m. This may be due to redistribution of volcaniclastic sediment from higher up the cone or, given the lack of T-phase signals during this period, the result of a slight mismatch between the two surveys in this area.

4.3 2013-2016

The 2013 to 2016 time-lapse covers a period of activity in July 2015 during which two clear T-phases were recorded (Robertson et al., 2015). Two landslides are observed, the first on the northern side of the crater rim is a further failure of the area from which the dome collapsed during the 1988 episode. This highly channelized collapse led to further deepening of the crater breach by up to 60m removing 2.29×10^6 m^3 of material. Down-dip this material was

redeposited, covering an area of $9.6x10^3 m^2$ with an average thickness of ~10m (note that some of this deposit likely extends outside the area of our study). The similarity of the 2013 and 2014 Nautilus surveys implies these changes occurred between October 2014 and February 2016.

The second major collapse on the SE flank of the volcano removed $4.36x10^6$ m^3 of material. The location of this collapse was surprising as the SE flank had previously been one of the most stable parts of the edifice (Dondin et al., 2017). A small volume from the backwall also contributed to this collapse as well as material from the edifice. This collapse is fairly deep (up to 66m) and steep sided. The steep sides and a sharp up-dip boundary of the associated deposit (see Figure 6, profile b), indicate that failure occurred as a fairly coherent slump.

During the 2015 event, seismic stations recorded two occurrences of sustained seismic tremor each of which lasted longer than an hour and were coincident with T-phase signals. At the time these were interpreted as indicators of sustained periods of eruption (Robertson et al., 2015). Given the lack of volcanic growth we suggest that these are more likely to be the real-time recordings of the landslides themselves. Hydroacoustic recordings of submarine landslides on a scale of several hours, have been previously reported from marine volcanoes such as Kilauea, Hawaii (Caplan-Auerbach et al., 2001).

In the case of the SE flank collapse in particular it is difficult to see how this could be an eruption triggered event, given its location away from the active vents within the KeJ crater (Carey et al., 2016). This collapse is likely the result of instabilities created by over-steepening of the flank of the volcano during the 1988 eruption and triggered by precursory seismic activity. The failure of the northern rim is more likely to have been triggered by eruption and volcanic loading. The morphology of this landslide is similar to those modelled by Acocella (2005) for loading of an unconsolidated cone (a good model for the volcanic sediment which forms much of the outer surface of KeJ).

4.4 2016-2017

The April 2017 seismic episode at KeJ lasted for 4 days from the 29th April until the 2nd May, and was again associated with several days of heightened seismicity, with the main T-phase signal on the morning of the 29th, lasting ~15m and consisting of 3 clear pulses (Latchman et al., 2017). The R.R.S. James Cook survey took place a few days later, on the morning of the 8th May, the shortest interval between a seismic signal and the following survey. As a result this should offer the most precise documentation of the effects of one of these events, since there was insufficient time for overprinting by erosion, sediment deposition or later activity.

In this time-lapse we observe what we interpret as the growth of a small lava dome (~25m high), a clear circular growth in the mouth of the breach in the northern rim of the crater. This eruption also led to the filling of much of the collapse scar created by the landslide in the previous time period by approximately 11m. This growth occurs in an identical location to the dome which formed in 1977 and suggests that there may still be an active volcanic conduit there. This interpretation is further supported by the imaging of active venting in the water column over this site detected during the 2017 R.R.S. James Cook survey (Figure 7). At the same time there is a drop in the central crater floor of up to 30m. We attribute this deflation as being caused by the expulsion of magma from the shallow interior of the cone. An alternative interpretation is that much of the central crater floor has collapsed through the breach in the crater rim, with the constructive signal purely the result of the redistribution of this material. Without ROV observations however it is difficult to know which of these scenarios is most likely.

There is also an extensive distributed swelling of the north-western flank of KeJ during this time interval. With a mean depth change of 8m this signal is only slightly above the 5m cut-off used on the data and cannot be easily attributed to any form of eruption given its separation from the active vents in the crater. We speculate that this signal may be the result of intrusion of magma at shallow depths on the flank of KeJ.

5 Discussion

5.1 T-phase episodes, morphological change and eruption history

During the study period we observe both positive and negative changes in the topography of KeJ. The most significant of these can be associated with reported volcanic T-phase signals. However, the bathymetric differences show that T-phase signals should not necessarily be equated to extrusive eruptions. The lack of evidence for significant addition of material, during the 2015 landslides in particular, means that T-phases produced by other processes should be considered. As well as being a direct recording of the landslides themselves these long duration T-phase signals could result from interactions between water and hot material uncovered by these landslides.

Many of the collapses take advantage of pre-existing weaknesses in the edifice of the volcano, with both the northern crater rim and the SW outer rim failing on more than one occasion during the study period. Landslides may be the result of over-steepening by previous eruptions, weakening by hydrothermal alteration, or structural weakening from previous collapses. Further loading during eruptions or shaking from seismic activity are probable triggers. Despite several previous collapses the SW flank of the cone in particular may still be gravitationally unstable (Dondin et al., 2017). The slump on the SE flank of the cone from the 2013-2016 time period may also still be unstable and liable to future failure.

Recent studies of Monowai (Kermadec arc) have observed a similar pattern of collapse structures that could be correlated with volcanic activity (Chadwick et al., 2008b; Watts et al., 2012; Wright et al., 2008). Regular collapses on a similar scale have also been recorded at NW Rota-1 in the Mariana arc (Chadwick et al., 2008a; Chadwick et al., 2012; Embley et al., 2006; Schnur et al., 2017). These small scale landslides (constituting fractions of a percent of the edifice's total volume and commonly 10s of meters deep) are increasingly being shown to play a key role in the long term evolution of submarine volcanoes, and the similarity in size and morphology of collapses from these three volcanoes, despite their locations in three markedly different island arcs is undeniable.

The volumes of documented collapses at KeJ are significantly smaller than would be considered a tsunami hazard. Taking Harbitz et al.'s (2012) work as a benchmark, (though it should be noted that these models consider an absolute worst case scenario) a collapse volume of $6x10^8 m^3$ could cause >6m waves on nearby Grenada and up to 1m as far away as Puerto Rico. Our biggest recorded collapse is only $2.18x10^7 m^3$, almost 30 times smaller than this amount. Nor do we see evidence for any large scale motion along the KeJ scarp which could be a precursor to a large sector collapse on the scale of the 43ka event. The total edifice today (measured down to the 600m contour) has a volume of $5.85x10^8 m^3$ ($0.585km^3$). In order to create a dangerous tsunami a large proportion of the cone would have to fail. Such a total failure seems highly unlikely without a significant episode of cone building and steepening of KeJ, or an explosive eruption on a scale which is historically unprecedented. Similar to the conclusions of Lindsay et al. (2005), we conclude that the tsunami risk associated with current

KeJ activity is quite low, given the current edifice configuration.

A strong disparity exists between the volumes of material being lost from the volcano in landslides and added to it as fresh deposits. Over the 1985-2017 time period, the calculated volume changes show $3.8x10^7$ m^3 was lost through collapses yet only around a fifth of this amount ($7.09x10^6$ m^3) was added as fresh volcanic deposits. Note that constructive anomalies which are clearly loose deposits resulting from collapses further up-structure (e.g. the two deposits in the 2013-2016 time period) are not included in these totals (see Table 2). Over the period of study, this gives a mean rate of magma output of $2.2x10^5$ m^3yr^{-1}. This is significantly less than the rate estimates of Devine and Sigurdsson (1995) of ~10^7 m^3yr^{-1} based on changes in the height of the volcanic cone between 1962 and 1978. These values were known to likely be an over-estimate due to being based on the erroneous 1962 H.M.S. Vidal bathymetric measurements (Lindsay et al., 2005).

The slow rate of magma production at KeJ results in a very different eruption style to that of Monowai, which during the period 2004-2007 quickly grew from 128mbsl to just 49mbsl (Watts et al., 2012) or NW Rota-1 which emitted $3.4x10^7m^3$ of volcaniclastic deposits in just 3 years between 2003 and 2009 (Chadwick et al., 2012). This is a similar volume to the total volume lost through mass wasting in 30 years at KeJ. In these other locations the volumetrics of collapses and eruptions are similar on a timescale of just a few years (Chadwick et al., 2008b; Schnur et al., 2017; Watts et al., 2012; Wright et al., 2008). Given that KeJ and Monowai are of comparable size (KeJ stands 1300m above the surrounding seafloor, Monowai 1000m) and summit depth (peak of KeJ ~190m b.s.l., Monowai 50-150m b.s.l.) this suggests fundamental differences between the eruption cycles at the two volcanoes. At KeJ this volume deficit is clearly not sustainable and we interpret that it must be capable of larger eruptions (or periods of much more intense activity) than those captured by this study. In order to fully balance out the material lost in the last 32 years would require the equivalent of an eruption depositing a 10m thick layer of material over the entire edifice all the way down to the 600m contour.

We conclude that constructive eruptions at KeJ are less frequent than previously thought. Cone construction occurs by infrequent eruptions and shallow emplacement events, rather than being a process which stays largely in step with collapse as observed elsewhere. Growth phases are interspersed with sustained periods of erosion and collapse driven by seismic activity and predominantly explosive eruptions which contribute little to the growth of the cone. The 1939 eruption is a likely candidate for one of these infrequent constructive episodes. The large ash cloud produced by this eruption that breached the ocean surface is certainly indicative of a much larger eruption than anything observed in recent decades (Devas, 1974). Despite the seeming regularity of eruptions, the majority of the historical events have contributed little in terms of constructive growth.

5.2 Implications for Hazard and Monitoring

The cyclical behaviour of eruptive episodes, interspersed with extended relatively quiescent periods lasting several decades and dominated by landslides and erosion is a behaviour similar to that recorded for many of the Antilles arc's subaerial volcanoes. La Soufrière (Guadeloupe) has experienced 6 major phreatic episodes since 1690 (the most recent in 1976-77), a repeat time of approximately 63 years (Feuillard et al., 1983; Jackson, 2013; Villemant et al., 2005). Soufrière, St. Vincent has also had a comparable eruption history (five major eruptions since 1718), with both episodes of dome building and phreatic explosions during that time (Heath et al., 1998a; Heath et al., 1998b). The eruption cycle at KeJ may be similar.

A sustained eruption would look very different seismologically to recent recordings. In particular we would expect a much higher number of T-phase events associated with any such prolonged eruption e.g. the May 2011 eruption of Monowai, which produced a total erupted volume of 8.75×10^6 m^3 (which would only satisfy about 1/4 of our observed construction deficit) was associated with 5 days of T-phase activity, with as many as 150 detected signals per day (Watts et al., 2012). In comparison, the 2015 episode at KeJ consisted of just two clear T-phase arrivals (Robertson et al., 2015). Activity associated with a larger event is likely to present a much more significant risk to shipping in the vicinity of the volcano. Large volume gas releases and more violent ejecta are likely, and a larger event could trigger higher volume landslides. We would hope that an eruption akin to the 1939 event would be almost immediately recognisable seismically as something of more major concern.

This study confirms the value of time-lapse bathymetry as a tool for monitoring submarine volcanoes. It should be noted this value is dramatically increased with the frequency of surveys. Where possible, if such a volcano is deemed a hazard, it is key that it is surveyed as soon as possible after any suspected activity. Coupled ROV surveys would also add a lot of additional information to what can be gleaned from bathymetry alone. Although this may be difficult given resources required it is the only way to accurately ground-truth the results of submarine volcanic activity. Even if a survey cannot be done immediately there is significant value to be gained by surveying the edifice before another volcanic episode can take place. As we saw with the 1985-2003 time-lapse, which contained 3 periods of T-phase activity, it can make interpretation of changes, and assigning these changes accurately to recorded events substantially more difficult.

Shallow water and proximity to shore may provide a number of possibilities for future monitoring of KeJ which would not be possible in less accessible locations. Autonomous underwater vehicles (AUVs) are increasingly being used to collect bathymetric data in a range of shallow water settings (Clague et al., 2011; Dupre et al., 2008; Grasmueck et al., 2006). Such a system could easily be launched from the shore near KeJ and would provide a relatively cheap means by which to conduct repeat bathymetric surveys compared to dedicated cruises. This would also have the advantage of being able to exactly repeat pre-programmed survey geometries. Alternatively KeJ would be a prime candidate for an underwater monitoring system, such as the Ocean Observatory Initiative's cabled array at Axial Seamount (Kelley et al., 2014) or the older HUGO system installed on Lo'ihi, Hawai'i in 1998(Caplan-Auerbach & Duennebier, 2001).

6 Conclusions

Through the analysis of six multibeam bathymetric surveys spanning the time period 1985-2017, we have identified a number of major morphological changes at the KeJ volcano in the southern Lesser Antilles with important implications for associated hazard. In doing so we have again demonstrated the value of time-lapse bathymetry for the monitoring of submarine volcanism.

- Morphological changes including dome construction, landslides and slumping can be correlated with T-phase signals at KeJ. This behaviour of morphological changes through regular, discrete, low-volume landslides is demonstrably similar to observations at other submarine arc volcanoes such as Monowai and NW Rota-1.
- T-phase signals are likely to have a range of sources including landslides rather than being solely the result of extrusive volcanism.

- During the period of study approximately 5 times more material was shed from the cone then was added to it by constructional volcanism.
- The repeat time of major eruptions at KeJ is likely to be on a longer timescale than previously thought. This is more similar to the behaviour of many of the sub-aerial volcanoes in the arc (e.g. La Soufrière, St. Vincent which erupts on an ~50 year cycle) because the regular decadal activity at KeJ has contributed little to the construction of the cone.
- In agreement with previous studies we conclude that tsunami risk associated with KeJ is minimal. The risk posed to shipping by ejected material and large gas releases during periods of eruption (particularly something on the scale of the 1939 event) should be the key hazard management concern.

Acknowledgements

This work was funded under NERC grant NE/K010743/1 and is project VOILA publication #4. We thank the captain, John Leask, officers, crew and science party members who sailed on R.R.S. James Cook cruises JC133 and JC149. Final processed grids used for the production of figures throughout the paper are available in the supplementary materials, unedited bathymetry datasets can be obtained on request from the British Oceanographic Data Centre (BODC). We also thank NOAA and the Ocean Exploration Trust for access to legacy datasets. RWA was supported by a PhD studentship funded by the NERC-Imperial SSCP DTP. Teledyne are also thanked for their flexibility in CARIS software licensing. We thank William Chadwick for his thoughtful review.

649

650

651

652

653

654

655

656

657

658

659

References

660 Acocella, V. (2005). Modes of sector collapse of volcanic cones: Insights from analogue experiments.
661 *Journal of Geophysical Research-Solid Earth*, 110(B2), 1-19. doi:10.1029/2004jb003166

662

663 Aki, K. & Ferrazzini, V. (2000). Seismic monitoring and modeling of an active volcano for prediction.
664 *Journal of Geophysical Research-Solid Earth*, 105(B7), 16617-16640. doi:10.1029/2000jb900033

665

666 Baldi, P., Bonvalot, S., Briole, P. & Marsella, M. (2000). Digital photogrammetry and kinematic GPS
667 applied to the monitoring of Vulcano Island, Aeolian Arc, Italy. *Geophysical Journal International*,
668 142(3), 801-811. doi:10.1046/j.1365-246x.2000.00194.x

669

670 Berry, C. (2017). *A time lapse study of the Kick 'em Jenny volcano, and an evaluation of its potential*
671 *hazards*. (Masters Thesis, MSci Geophysics). London, UK: Imperial College London, Department of
672 Earth Science and Engineering. Available via Research Gate. doi:10.13140/RG.2.2.25489.12645.

673

674 Bohnenstiehl, D. R., Dziak, R. P., Matsumoto, H. & Lau, T. K. A. (2013). Underwater acoustic records
675 from the March 2009 eruption of Hunga Ha'apai-Hunga Tonga volcano in the Kingdom of Tonga.
676 *Journal of Volcanology and Geothermal Research*, 249 12-24. doi:10.1016/j.jvolgeores.2012.08.014

677

678 Bonaccorso, A., Aloisi, M. & Mattia, M. (2002). Dike emplacement forerunning the Etna July 2001
679 eruption modeled through continuous tilt and GPS data. *Geophysical Research Letters*, 29(13), 1-4.
680 doi:10.1029/2001gl014397

681

682 Bonaccorso, A., Calvari, S., Linde, A., Sacks, S. & Boschi, E. (2012). Dynamics of the shallow plumbing
683 system investigated from borehole strainmeters and cameras during the 15 March, 2007 Vulcanian
684 paroxysm at Stromboli volcano. *Earth and Planetary Science Letters*, 357 249-256.
685 doi:10.1016/j.epsl.2012.09.009

686

687

688 Boudon, G., Le Friant, A., Komorowski, J. C., Deplus, C. & Semet, M. P. (2007). Volcano flank
689 instability in the Lesser Antilles arc: Diversity of scale, processes, and temporal recurrence. *Journal of*
690 *Geophysical Research-Solid Earth*, 112(B8), 1-28. doi:10.1029/2006jb004674

691
692 Bouysse, P. (1988). Opening of the Grenada Back-Arc Basin and Evolution of the Caribbean Plate
693 during the Mesozoic and Early Paleogene. *Tectonophysics*, 149(1-2), 121-143.
694 doi:10.1016/0040-1951(88)90122-9

695
696 Bouysse, P., Mascle, A., Mauffret, A., Delepinay, B. M., Jany, I., Leclere-Vanhoeve, A. & Montjaret, M.
697 C. (1988). Submarine Tectonic and Volcanic Structures of the Lesser Antilles Recent Arc (Kick'em
698 Jenny, Qualibou, Mount Pelee, Northwest Guadeloupe). *Marine Geology*, 81(1-4), 261-287.
699 doi:10.1016/0025-3227(88)90031-X

700
701 Bouysse, P. & Westercamp, D. (1990). Subduction of Atlantic aseismic ridges and Late Cenozoic
702 Evolution of the Lesser Antilles Island-Arc. *Tectonophysics*, 175(4), 349-380.
703 doi:10.1016/0040-1951(90)90180-G

704
705 Brenguier, F., Shapiro, N. M., Campillo, M., Ferrazzini, V., Duputel, Z., Coutant, O. & Nercessian, A.
706 (2008). Towards forecasting volcanic eruptions using seismic noise. *Nature Geoscience*, 1(2),
707 126-130. doi:10.1038/ngeo104

708
709 Budetta, G., Carbone, D. & Greco, F. (1999). Subsurface mass redistributions at Mount Etna (Italy)
710 during the 1995-1996 explosive activity detected by microgravity studies. *Geophysical Journal*
711 *International*, 138(1), 77-88. doi:10.1046/j.1365-246x.1999.00836.x

712
713 Caplan-Auerbach, J. & Duennebier, F. (2001). Seismic and acoustic signals detected at Lo'ihi
714 Seamount by the Hawai'i Undersea Geo-Observatory. *Geochemistry Geophysics Geosystems*, 2.
715 doi:10.1029/2000GC000113

716
717 Caplan-Auerbach, J., Fox, C. G. & Duennebier, F. K. (2001). Hydroacoustic detection of submarine
718 landslides on Kilauea volcano. *Geophysical Research Letters*, 28(9), 1811-1813.
719 doi:10.1029/2000gl012545

720
721 Carey, S., Ballard, R., Bell, K. L. C., Bell, R. J., Connally, P., Dondin, F., . . . Smart, C. (2014). Cold seeps
722 associated with a submarine debris avalanche deposit at Kick'em Jenny volcano, Grenada (Lesser
723 Antilles). *Deep-Sea Research Part I-Oceanographic Research Papers*, 93 156-160.
724 doi:10.1016/j.dsr.2014.08.002

725
726 Carey, S., Olsen, R., Bell, K. L. C., Ballard, R., Dondin, F., Roman, C., . . . Moyer, C. (2016).
727 Hydrothermal venting and mineralization in the crater of Kick'em Jenny submarine volcano, Grenada
728 (Lesser Antilles). *Geochemistry Geophysics Geosystems*, 17(3), 1000-1019.
729 doi:10.1002/2015GC006060

730
731 Cashman, K. V. & Sparks, R. S. J. (2013). How volcanoes work: A 25 year perspective. *Geological*
732 *Society of America Bulletin*, 125(5-6), 664-690. doi:10.1130/B30720.1

Chadwick, W. W., Cashman, K. V., Embley, R. W., Matsumoto, H., Dziak, R. P., de Ronde, C. E. J., . . . Merle, S. G. (2008a). Direct video and hydrophone observations of submarine explosive eruptions at NW Rota-1 volcano, Mariana arc. *Journal of Geophysical Research-Solid Earth*, 113(B8), 1-23. doi:10.1029/2007jb005215

Chadwick, W. W., Dziak, R. P., Haxel, J. H., Embley, R. W. & Matsumoto, H. (2012). Submarine landslide triggered by volcanic eruption recorded by in situ hydrophone. *Geology*, 40(1), 51-54. 10.1130/G32495.1

Chadwick, W. W., Merle, S. G., Buck, N. J., Lavelle, J. W., Resing, J. A. & Ferrini, V. (2014). Imaging of CO2 bubble plumes above an erupting submarine volcano, NW Rota-1, Mariana Arc. *Geochemistry Geophysics Geosystems*, 15(11), 4325-4342. doi:10.1002/2014GC005543

Chadwick, W. W., Wright, I. C., Schwarz-Schampera, U., Hyvernaud, O., Reymond, D. & de Ronde, C. E. J. (2008b). Cyclic eruptions and sector collapses at Monowai submarine volcano, Kermadec arc: 1998-2007. *Geochemistry Geophysics Geosystems*, 9(10), 1-17. doi:10.1029/2008gc002113

Chiarabba, C., Amato, A., Boschi, E. & Barberi, F. (2000). Recent seismicity and tomographic modeling of the Mount Etna plumbing system. *Journal of Geophysical Research-Solid Earth*, 105(B5), 10923-10938. doi:10.1029/1999jb900427

Clague, D. A., Paduan, J. B., Caress, D. W., Thomas, H., Chadwick, W. W. & Merle, S. G. (2011). Volcanic morphology of West Mata Volcano, NE Lau Basin, based on high-resolution bathymetry and depth changes. *Geochemistry Geophysics Geosystems*, 12(11), 1-21. doi:10.1029/2011gc003791

Del Negro, C., Currenti, G., Napoli, R. & Vicari, A. (2004). Volcanomagnetic changes accompanying the onset of the 2002-2003 eruption of Mt. Etna (Italy). *Earth and Planetary Science Letters*, 229(1-2), 1-14. doi:10.1016/j.epsl.2004.10.033

Del Negro, C., Napoli, R. & Sicali, A. (2002). Automated system for magnetic monitoring of active volcanoes. *Bulletin of Volcanology*, 64(2), 94-99. doi:10.1007/s00445-001-0186-x

Deplus, C., Le Friant, A., Boudon, G., Komorowski, J. C., Villemant, B., Harford, C., . . . Cheminee, J. L. (2001). Submarine evidence for large-scale debris avalanches in the Lesser Antilles Arc. *Earth and Planetary Science Letters*, 192(2), 145-157. doi:10.1016/S0012-821x(01)00444-7

Devas, R. P. (1974). A History of the Island of Grenada, 1498-1796, with Some Notes and Comments on Carriacou and Events of Later Years. *Carenage Press*, St. George's, Grenada.

Devine, J. D. & Sigurdsson, H. (1995). Petrology and eruption styles of Kick'em-Jenny submarine volcano, Lesser Antilles island arc. *Journal of Volcanology and Geothermal Research*, 69(1-2), 35-58. doi:10.1016/0377-0273(95)00025-9

777 Diefenbach, A. K., Crider, J. G., Schilling, S. P. & Dzurisin, D. (2012). Rapid, low-cost photogrammetry
778 to monitor volcanic eruptions: an example from Mount St. Helens, Washington, USA. *Bulletin of*
779 *Volcanology*, 74(2), 579-587. doi:10.1007/s00445-011-0548-y

780

781 Dondin, F., Lebrun, J. F., Kelfoun, K., Fournier, N. & Randrianasolo, A. (2012). Sector collapse at Kick
782 'em Jenny submarine volcano (Lesser Antilles): numerical simulation and landslide behaviour.
783 *Bulletin of Volcanology*, 74(2), 595-607. doi:10.1007/s00445-011-0554-0

784

785 Dondin, F. J. Y., Heap, M. J., Robertson, R. E. A., Dorville, J. F. M. & Carey, S. (2017). Flank instability
786 assessment at Kick-'em-Jenny submarine volcano (Grenada, Lesser Antilles): a multidisciplinary
787 approach using experiments and modeling. *Bulletin of Volcanology*, 79(1), 1-15.
788 doi:10.1007/S00445-016-1090-8

789

790 Druitt, T. H. & Kokelaar, B. P. (2002). The Eruption of Soufrière Hills Volcano, Montserrat, from 1995
791 to 1999. *Geological Society of London*, London, UK.

792

793 Duffell, H. J., Oppenheimer, C., Pyle, D. M., Galle, B., McGonigle, A. J. S. & Burton, M. R. (2003).
794 Changes in gas composition prior to a minor explosive eruption at Masaya volcano, Nicaragua.
795 *Journal of Volcanology and Geothermal Research*, 126(3-4), 327-339.
796 doi:10.1016/S0377-0273(03)00156-2

797

798 Dupre, S., Buffet, G., Mascle, J., Foucher, J. P., Gauger, S., Boetius, A., . . . Party, B. S. (2008).
799 High-resolution mapping of large gas emitting mud volcanoes on the Egyptian continental margin
800 (Nile Deep Sea Fan) by AUV surveys. *Marine Geophysical Research*, 29(4), 275-290.
801 doi:10.1007/s11001-009-9063-3

802

803 Dziak, R. P. & Fox, C. G. (1999). The January 1998 earthquake swarm at axial volcano, Juan de Fuca
804 Ridge: Hydroacoustic evidence of seafloor volcanic activity. *Geophysical Research Letters*, 26(23),
805 3429-3432. Doi 10.1029/1999gl002332

806

807 Dzurisin, D. (2003). A comprehensive approach to monitoring volcano deformation as a window on
808 the eruption cycle. *Reviews of Geophysics*, 41(1), 1-29. doi:10.1029/2001rg000107

809

810 Edmonds, M., Oppenheimer, C., Pyle, D. M., Herd, R. A. & Thompson, G. (2003). SO_2 emissions from
811 Soufriere Hills Volcano and their relationship to conduit permeability, hydrothermal interaction and
812 degassing regime. *Journal of Volcanology and Geothermal Research*, 124(1-2), 23-43.
813 doi:10.1016/S0377-0273(03)00041-6

814

815 Embley, R. W., Chadwick, W. W., Baker, E. T., Butterfield, D. A., Resing, J. A., De Ronde, C. E. J., . . .
816 Tamura, Y. (2006). Long-term eruptive activity at a submarine arc volcano. *Nature*, 441(7092),
817 494-497. doi:10.1038/nature04762

818

819 Embley, R. W., Merle, S. G., Baker, E. T., Rubin, K. H., Lupton, J. E., Resing, J. A., . . . Baumberger, T.
820 (2014). Eruptive modes and hiatus of volcanism at West Mata seamount, NE Lau basin: 1996-2012.
821 *Geochemistry Geophysics Geosystems*, 15(10), 4093-4115. 10.1002/2014GC005387

Feuillard, M., Allegre, C. J., Brandeis, G., Gaulon, R., Lemouel, J. L., Mercier, J. C., . . . Semet, M. P. (1983). The 1975-1977 Crisis of La Soufriere De Guadeloupe (F.W.I): a Still-Born Magmatic Eruption. *Journal of Volcanology and Geothermal Research*, 16(3-4), 317-334. doi:10.1016/0377-0273(83)90036-7

Fiske, R. S., Cashman, K. V., Shibata, A. & Watanabe, K. (1998). Tephra dispersal from Myojinsho, Japan, during its shallow submarine eruption of 1952-1953. *Bulletin of Volcanology*, 59(4), 262-275. doi:10.1007/s004450050190

Fiske, R. S. & Shepherd, J. B. (1990). 12 Years of Ground-Tilt Measurements on the Soufriere of St-Vincent, 1977-1989. *Bulletin of Volcanology*, 52(3), 227-241. doi:10.1007/Bf00334806

Gisler, G., Weaver, R. & Gittings, M. L. (2006). Two-Dimensional simulations of explosive eruptions of Kick-em Jenny and other submarine volcanos. *Science of Tsunami Hazards*, 25(1), 34-41.

Graff, J. R., Blake, J. A. & Wishner, K. F. (2008). A new species of Malacoceros (Polychaeta : Spionidae) from Kick'em Jenny, a hydrothermally active submarine volcano in the Lesser Antilles Arc. *Journal of the Marine Biological Association of the United Kingdom*, 88(5), 925-930. doi:10.1017/S0025315408001884

Grasmueck, M., Eberli, G. P., Viggiano, D. A., Correa, T., Rathwell, G. & Luo, J. G. (2006). Autonomous underwater vehicle (AUV) mapping reveals coral mound distribution, morphology, and oceanography in deep water of the Straits of Florida. *Geophysical Research Letters*, 33(23), 1-6. doi:10.1029/2006gl027734

Harbitz, C. B., Glimsdal, S., Bazin, S., Zamora, N., Lovholt, F., Bungum, H., . . . Kjekstad, O. (2012). Tsunami hazard in the Caribbean: Regional exposure derived from credible worst case scenarios. *Continental Shelf Research*, 38 1-23. doi:10.1016/j.csr.2012.02.006

Heath, E., MacDonald, R., Belkin, H., Hawkesworth, C. & Sigurdsson, H. (1998a). Magmagenesis at Soufriere Volcano, St Vincent, Lesser Antilles arc. *Journal of Petrology*, 39(10), 1721-1764. doi:10.1093/petrology/39.10.1721

Heath, E., Turner, S. P., Macdonald, R., Hawkesworth, C. J. & van Calsteren, P. (1998b). Long magma residence times at an island arc volcano (Soufriere, St. Vincent) in the Lesser Antilles: evidence from ^{238}U-^{230}Th isochron dating *Earth and Planetary Science Letters*, 163(1-4), 413-413.

Ito, A., Sugioka, H., Suetsugu, D., Shiobara, H., Kanazawa, T. & Fukao, Y. (2012). Detection of small earthquakes along the Pacific-Antarctic Ridge from T-waves recorded by abyssal ocean-bottom observatories. *Marine Geophysical Research*, 33(3), 229-238. doi:10.1007/s11001-012-9158-0

Jackson, P., Shepherd, J. B., Robertson, R. E. A. & Skerritt, G. (1998). Ground deformation studies at Soufriere Hills Volcano, Montserrat I: Electronic distance meter studies. *Geophysical Research Letters*, 25(18), 3409-3412. doi:10.1029/98gl01656

Jackson, T. A. (2013). A review of volcanic island evolution and magma production rate: an example from a Cenozoic island arc in the Caribbean. *Journal of the Geological Society*, 170(3), 547-556. doi:10.1144/jgs2011-166

Kelley, D. S., Delaney, J. R. & Juniper, S. K. (2014). Establishing a new era of submarine volcanic observatories: Cabling Axial Seamount and the Endeavour Segment of the Juan de Fuca Ridge. *Marine Geology*, 352 426-450. 10.1016/j.margeo.2014.03.010

Koschinsky, A., Seifert, R., Knappe, A., Schmidt, K. & Halbach, P. (2007). Hydrothermal fluid emanations from the submarine Kick'em Jenny volcano, Lesser Antilles island arc. *Marine Geology*, 244(1-4), 129-141. doi:10.1016/j.margeo.2007.06.013

Latchman, J. L., Robertson, R. E. A., Lynch, L. L., Dondin, F., Ramsingh, C., Stewart, R., . . . Madoo, F. (2017). 2017/04/29 Eruption of Kick-'em-Jenny Submarine Volcano. The UWI Seismic Research Centre, St Augustine, Trinidad and Tobago, pp. 1-29. http://uwiseismic.com/Downloads/20170711_Kick-em-Jenny_20170429_Eruption_VOLC1.pdf.

Lindsay, J. M., Shepherd, J. B. & Wilson, D. (2005). Volcanic and scientific activity at Kick'em Jenny submarine volcano 2001-2002: Implications for volcanic hazard in the Southern Grenadines, Lesser Antilles. *Natural Hazards*, 34(1), 1-24. doi:10.1007/s11069-004-1566-2

Maeno, F., Nakada, S. & Kaneko, T. (2016). Morphological evolution of a new volcanic islet sustained by compound lava flows. *Geology*, 44(4), 259-262. doi:10.1130/G37461.1

Massonnet, D., Briole, P. & Arnaud, A. (1995). Deflation of Mount Etna Monitored by Spaceborne Radar Interferometry. *Nature*, 375(6532), 567-570. doi:10.1038/375567a0

Massonnet, D. & Feigl, K. L. (1998). Radar interferometry and its application to changes in the earth's surface. *Reviews of Geophysics*, 36(4), 441-500. doi:10.1029/97rg03139

McClelland, L., Duncker, K. & Hoppe, K. (1989). Kick-'em-Jenny Volcano. *Smithsonian Institution, Scientific Event Alert Network Bulletin*, 14(5), 12.

McClelland, L., Summers, M. & Duncker, K. (1988). Kick-'em-Jenny Volcano. *Smithsonian Institution, Scientific Event Alert Network Bulletin*, 13(12), 9.

Metz, D., Watts, A. B., Grevemeyer, I., Rodgers, M. & Paulatto, M. (2016). Ultra-long-range hydroacoustic observations of submarine volcanic activity at Monowai, Kermadec Arc. *Geophysical Research Letters*, 43(4), 1529-1536. doi:10.1002/2015GL067259

Moore, J. G. (1985). Structure and eruptive mechanisms at Surtsey Volcano, Iceland. *Geological Magazine*, 122(6), 649-661.

911 Paris, R., Switzer, A. D., Belousova, M., Belousov, A., Ontowirjo, B., Whelley, P. L. & Ulvrova, M.
912 (2014). Volcanic tsunami: a review of source mechanisms, past events and hazards in Southeast Asia
913 (Indonesia, Philippines, Papua New Guinea). *Natural Hazards*, 70(1), 447-470.
914 doi:10.1007/s11069-013-0822-8

915
916 Parks, M. M., Biggs, J., England, P., Mather, T. A., Nomikou, P., Palamartchouk, K., . . . Zacharis, V.
917 (2012). Evolution of Santorini Volcano dominated by episodic and rapid fluxes of melt from depth.
918 *Nature Geoscience*, 5(10), 749-754. doi:10.1038/NGEO1562

919
920 Puglisi, G. & Bonforte, A. (2004). Dynamics of Mount Etna Volcano inferred from static and kinematic
921 GPS measurements. *Journal of Geophysical Research-Solid Earth*, 109(B11), 1-15.
922 doi:10.1029/2003jb002878

923
924 Puglisi, G., Bonforte, A. & Maugeri, S. R. (2001). Ground deformation patterns on Mount Etna, 1992
925 to 1994, inferred from GPS data. *Bulletin of Volcanology*, 62(6-7), 371-384.
926 doi:10.1007/s004450000112

927
928 Resing, J. A., Rubin, K. H., Embley, R. W., Lupton, J. E., Baker, E. T., Dziak, R. P., . . . Thomas, H. (2011).
929 Active submarine eruption of boninite in the northeastern Lau Basin. *Nature Geoscience*, 4(11),
930 799-806. 10.1038/NGEO1275

931
932 Ricco, C., Aquino, I., Borgstrom, S. E. P. & Del Gaudio, C. (2013). 19 years of tilt data on Mt. Vesuvius:
933 state of the art and future perspectives. *Annals of Geophysics*, 56(4), 1-20. doi:10.4401/Ag-6459

934
935 Robertson, R. E. A., Latchman, J. L., Lynch, L., Dondin, F., Ash, C., Camejo, M., . . . Stinton, A. (2015).
936 Report on the 2015 Unrest Activity at Kick-'em-Jenny Submarine Volcano, Grenada. The UWI Seismic
937 Research Centre, St Augustine, Trinidad and Tobago, pp. 1-20.
938 http://uwiseismic.com/Downloads/KeJReport2015.pdf.

939
940 Rubin, K. H., Soule, S. A., Chadwick, W. W., Fornari, D. J., Clague, D. A., Embley, R. W., . . . Dziak, R. P.
941 (2012). Volcanic Eruptions in the Deep Sea. *Oceanography*, 25(1), 142-157.
942 10.5670/oceanog.2012.12

943
944 Rymer, H. (1994). Microgravity change as a precursor to volcanic activity. *Journal of Volcanology and*
945 *Geothermal Research*, 61(3-4), 311-328. doi:10.1016/0377-0273(94)90011-6

946
947 Schnur, S. R., Chadwick, W. W., Embley, R. W., Ferrini, V. L., de Ronde, C. E. J., Cashman, K. V., . . .
948 Matsumoto, H. (2017). A decade of volcanic construction and destruction at the summit of NW
949 Rota-1 seamount: 2004-2014. *Journal of Geophysical Research-Solid Earth*, 122(3), 1558-1584.
950 doi:10.1002/2016JB013742

951
952 Shepherd, J. B. & Robson, R. B. (1967). The source of the T-Phase recorded in the Eastern Caribbean
953 on October 24, 1965. *Bulletin of the Seismological Society of America*, 57(2), 227-234.

954

955 Sigurdsson, H. & Shepherd, J. B. (1974). Amphibole-bearing basalts from the submarine volcano Kick
956 'em Jenny in the Lesser Antilles island arc. *Bull. Volc.*, 37 891-910.

957
958 Smith, M. S. & Shepherd, J. B. (1996). Tsunami waves generated by volcanic landslides: An
959 assessment of the hazard associated with Kick 'em Jenny. *Volcano Instability on the Earth and Other*
960 *Planets*,(110), 115-123.

961
962 Sparks, R. S. J. (2003). Forecasting volcanic eruptions. *Earth and Planetary Science Letters*, 210(1-2),
963 1-15. doi:10.1016/S0012-821x(03)00124-9

964
965 Symithe, S., Calais, E., de Chabalier, J. B., Robertson, R. & Higgins, M. (2015). Current block motions
966 and strain accumulation on active faults in the Caribbean. *Journal of Geophysical Research-Solid*
967 *Earth*, 120(5), 3748-3774. doi:10.1002/2014JB011779

968
969 Villemant, B., Hammouya, G., Michel, A., Semet, M. P., Komorowski, J. C., Boudon, G. & Cheminee, J.
970 L. (2005). The memory of volcanic waters: Shallow magma degassing revealed by halogen
971 monitoring in thermal springs of La Soufriere volcano (Guadeloupe, Lesser Antilles). *Earth and*
972 *Planetary Science Letters*, 237(3-4), 710-728. doi:10.1016/j.epsl.2005.05.013

973
974 Voight, B., Hidayat, D., Sacks, S., Linde, A., Chardot, L., Clarke, A., . . . Young, S. R. (2010). Unique
975 strainmeter observations of Vulcanian explosions, Soufriere Hills Volcano, Montserrat, July 2003.
976 *Geophysical Research Letters*, 37 1-5. doi:10.1029/2010gl042551

977
978 Wadge, G., Voight, B., Sparks, R. S. J., Cole, P. D., Loughlin, S. C. & Robertson, R. E. A. (2014). An
979 overview of the eruption of Soufrière Hills Volcano, Montserrat from 2000 to 2010. *In*: G. Wadge,
980 R.E.A. Robertson & B. Voight (Eds) 2014: The Eruption of Soufriere Hills Volcano, Montserrat from
981 2000 to 2010, Geological Society Memoirs. *The Geological Society of London*, London, UK.

982
983 Watlington, R. A., Wilson, W. D., Johns, W. E. & Nelson, C. (2002). Updated bathymetric survey of
984 Kick-'em-Jenny submarine volcano. *Marine Geophysical Researches*, 23(3), 271-276.
985 doi:10.1023/A:1023615529336

986
987 Watt, S. F. L., Talling, P. J., Vardy, M. E., Heller, V., Huhnerbach, V., Urlaub, M., . . . Maeno, F. (2012a).
988 Combinations of volcanic-flank and seafloor-sediment failure offshore Montserrat, and their
989 implications for tsunami generation. *Earth and Planetary Science Letters*, 319 228-240.
990 doi:10.1016/j.epsl.2011.11.032

991
992 Watt, S. F. L., Talling, P. J., Vardy, M. E., Masson, D. G., Henstock, T. J., Huhnerbach, V., . . . Karstens,
993 J. (2012b). Widespread and progressive seafloor-sediment failure following volcanic debris
994 avalanche emplacement: Landslide dynamics and timing offshore Montserrat, Lesser Antilles.
995 *Marine Geology*, 323 69-94. doi:10.1016/j.margeo.2012.08.002

996
997 Watts, A. B., Nomikou, P., Moore, J. D. P., Parks, M. M. & Alexandri, M. (2015). Historical
998 bathymetric charts and the evolution of Santorini submarine volcano, Greece. *Geochemistry*
999 *Geophysics Geosystems*, 16(3), 847-869. doi:10.1002/2014GC005679

Watts, A. B., Peirce, C., Grevemeyer, I., Paulatto, M., Stratford, W., Bassett, D., . . . de Ronde, C. E. J. (2012). Rapid rates of growth and collapse of Monowai submarine volcano in the Kermadec Arc. *Nature Geoscience*, 5(7), 510-515. doi:10.1038/ngeo1473

Wishner, K. F., Graff, J. R., Martin, J. W., Carey, S., Sigurdsson, H. & Seibel, B. A. (2005). Are midwater shrimp trapped in the craters of submarine volcanoes by hydrothermal venting? *Deep-Sea Research Part I-Oceanographic Research Papers*, 52(8), 1528-1535. doi:10.1016/j.dsr.2005.03.012

Wright, I. C., Chadwick, W. W., de Ronde, C. E. J., Reymond, D., Hyvernaud, O., Gennerich, H. H., . . . Bannister, S. C. (2008). Collapse and reconstruction of Monowai submarine volcano, Kermadec arc, 1998-2004. *Journal of Geophysical Research-Solid Earth*, 113(B8), 1-13. doi:10.1029/2007jb005138

Figure 1. Map showing location of Kick-‘em-Jenny in the southern Lesser Antilles. Bathymetry comes from the 2013 R/V Nautilus dataset in the main map and GEBCO in the inset. The cone of KeJ can be clearly observed within the large horseshoe shaped collapse scarp, located on the western flank of the arc.

Figure 2. Timeline of bathymetric surveys and recorded T-phase episodes at KeJ. Depth values for the peak of KeJ are taken from the compilation of Lindsay et al., (2005) where original data sources were unavailable. Stars indicate multibeam bathymetry datasets used in this study. Note that depth measurements refer to the single shallowest point on KeJ from that survey, in most cases this is the rim of the crater, but for the R/V Endeavour (1978), N.O. Noroit (1981) and R/V Conrad (1985) it is the peak of a volcanic dome on the northern side of the crater.

Figure 3. 3D projection of KeJ bathymetry using R/V Nautilus (2013) bathymetric dataset. Viewpoint is from an azimuth of 205°. 1) Horseshoe shaped scarp surrounding KeJ, the result of the collapse of a larger “Proto-Jenny” at 43ka (Dondin et al., 2017). 2) Active cone of KeJ. 3) Kick-‘em-Jack, the largest of the volcanic cones in the back-wall above KeJ. 4) Deposit from the 43Ka collapse of “Proto-Jenny”. Kick-‘em-Jenny has subsequently grown through this debris flow. 5) Run out of the debris flow extends for up to 14km into the deep water of the Grenada Basin.

Cruise	Vessel	Instrument Make	Model	Frequency (kHz)	Beams per Ping	Mean Survey Speed (Knots)	Maximum Theoretical Swath Width (m) (x Water Depth)	Mean Standard Deviation of Cells in Final Grid (m)	Depth Shift Relative to final R/V Nautilus 2013 grid*
1985	R/V Robert D. Conrad	General Instrument Corporation	SeaBeam	12	19	5.2	3.0	-	-1.5
2003	R/V Ronald H. Brown	Sea Beam Instruments Inc.	SeaBeam 2112	12	120	6.4	3.4	7.8	-0.35
2013	R/V Nautilus	Kongsberg	EM302	30	432	7.8	5.5	1.1	0
2014	R/V Nautilus	Kongsberg	EM302	30	432	9.2	5.5	1.1	0
2016	R.R.S. James Cook	Kongsberg	EM710	70-100	200	5.0	5.5	2.2	+0.5
2017	R. R. S. James Cook	Kongsberg	EM710	70-100	200	5.0	5.5	3.8	+2.1

Table 1. Survey statistics of the bathymetric datasets and final grids used in the study. Mean survey velocities were calculated from the timing/location data within each dataset. Maximum theoretical swath width is calculated based on the maximum possible beam angle for each system. Following processing the true swath width is likely to be significantly less than this (due to the lower precision of the outer, high angle soundings). Standard deviation values for each grid were calculated as part of the gridding process in CARIS/HIPS. Each grid has a cell size of 5m, except for the 1985 survey which has a cell size of 30m. More detailed maps of the standard deviation in each cell and the sounding density for each grid can be found in the supplementary materials. *Positive values correspond to an upwards shift i.e. the surface was initially deeper than the R/V Nautilus (2013) grid.

Figure 4. Final bathymetric grids produced following reprocessing of legacy bathymetry datasets. Surfaces shown have been smoothed using a 50m filter for the purposes of display. The unsmoothed 5m grids are used for all depth change calculations discussed in the paper and differences shown in Figure 5.All surfaces are contoured at 25m intervals. For survey parameters associated with each grid see Table 1.

Figure 5. Depth-difference images calculated from final bathymetric grids. Cleaned difference grids (red-blue scale) are shown on top of the latter of the two bathymetric grids used in the time-lapse (grey scale). Labelled morphological changes correspond to volumes shown in Table 2.

Description	Time-lapse	Maximum Depth Change (m)	Mean Depth Change (m)	Volume Change ($x10^6m^3$)
SW Flank Volcanic Spine Collapse	1985-2003	-174.62	-58.47	-21.8
S Crater Rim Growth	1985-2003	+86.95	+48.98	+4.26
N Crater Rim Dome Collapse	1985-2003	-82.90	-44.90	-2.48
NW Flank Collapse	1985-2003	-70.01	-42.20	-4.62
SW Flank Wasting	2003-2013	-26.84	-7.25	-1.88
N Crater Rim Collapse	2013-2016	-59.61	-18.45	-2.29
N Collapse Deposit	2013-2016	+23.50	+11.20	+1.12*
SE Flank Collapse	2013-2016	-65.88	-21.36	-4.36
SE Flank Slump Deposit	2013-2016	+27.59	+10.34	+5.74*
N Crater Rim Dome Growth and Flow	2016-2017	+35.66	+10.50	+0.59
Central Crater Collapse	2016-2017	-37.11	-13.13	-0.94
NW Flank Swell	2016-2017	+32.95	+8.04	+2.24
			Net Total:	-31.28

Table 2. Volume changes calculated from cleaned difference grids over KeJ. These grids with labelled morphological changes can be seen in Figure 5. The total positive (addition of material) volume gain is $7.09x10^6m^3$. The total negative (loss of material) volume decrease is $-38.37x10^6m^3$. *These positive changes are clearly deposits corresponding to up-slope collapses during this time period as such they have not been included in the total volume balance shown.

Figure 6. Profiles through final bathymetric grids over KeJ. Note that due to the relatively minor changes between 2003 and 2013, the 2003 survey is not shown for the sake of simplicity. Values in brackets refer to the year(s) in which a given feature was present.

Figure 7. 2017 EM710 multibeam bathymetry and water column data. Gas plumes shown were visible as backscatter anomalies in the water column data and were extracted using the software FM Midwater before being rendered in 3D using IVS Fledermaus. Similar methodology was used by Chadwick et al. (2014) in imaging gas plumes over NW Rota-1. As well as the expected gas plumes from vents in the crater floor, we also observe a plume being emitted from a vent on the outer western crater rim. This Fledermaus scene is available to view via the supplementary material.

Figure 1.

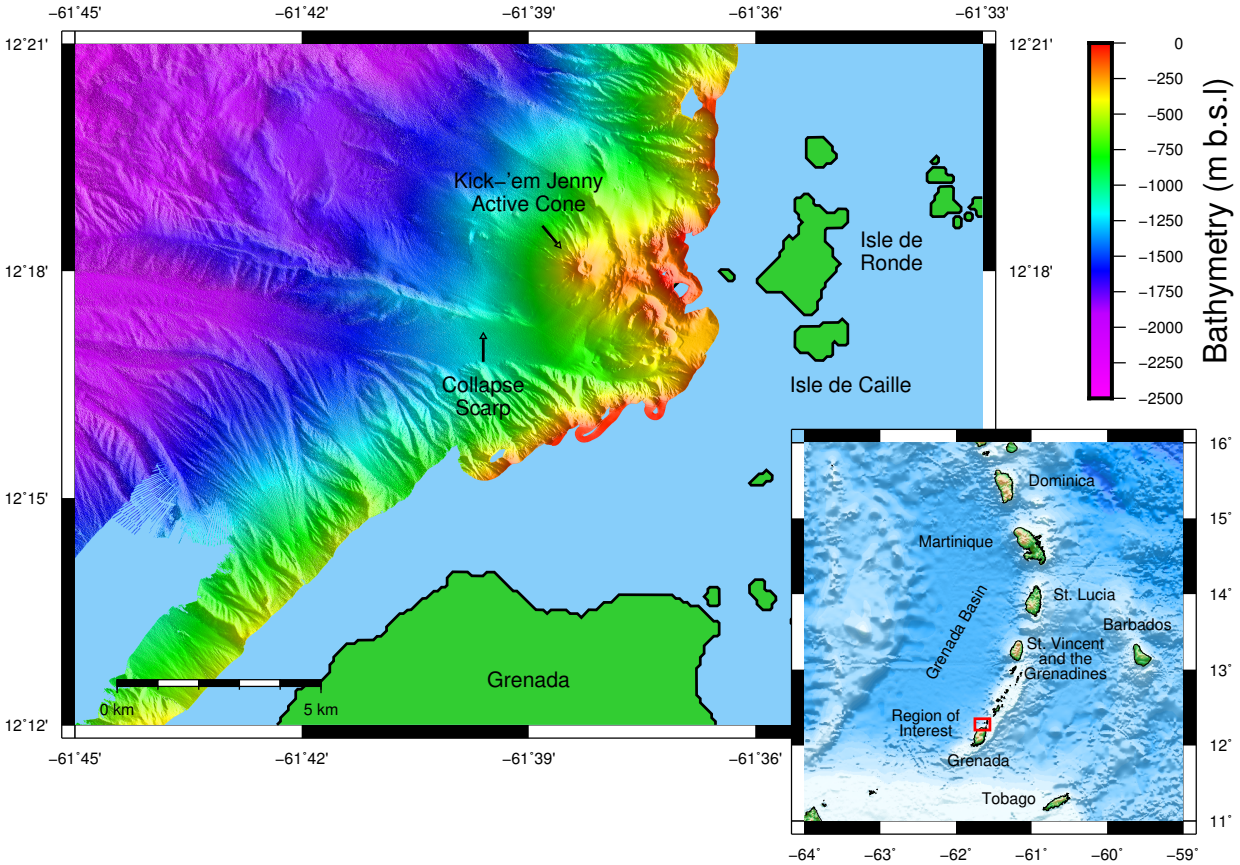
−61˚45'
−61˚42'
−61˚39'
−61˚36'
−61˚33'
12˚21'
12˚18'
12˚15'
12˚12'
Kick–'em Jenny
Active Cone
Collapse
Scarp
Isle de
Ronde
Isle de Caille
Grenada
0 km
5 km
0
−250
−500
−750
−1000
−1250
−1500
−1750
−2000
−2250
−2500
Bathymetry (m b.s.l)
Dominica
Martinique
St. Lucia
Barbados
St. Vincent
and the
Grenadines
Grenada Basin
Region of
Interest
Grenada
Tobago
16˚
15˚
14˚
13˚
12˚
11˚
−64˚
−63˚
−62˚
−61˚
−60˚
−59˚

Figure 2.

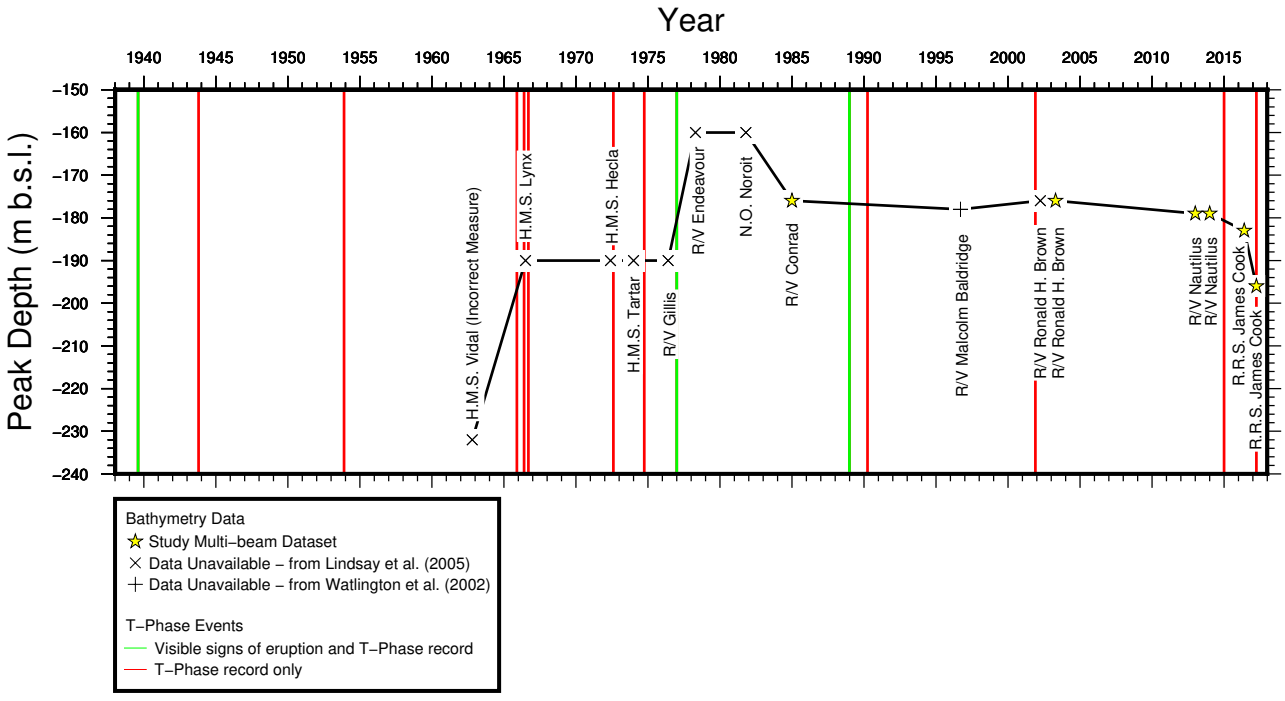
Year
1940
1945
1950
1955
1960
1965
1970
1975
1980
1985
1990
1995
2000
2005
2010
2015
Peak Depth (m b.s.l.)
−150
−160
−170
−180
−190
−200
−210
−220
−230
−240
H.M.S. Vidal (Incorrect Measure)
H.M.S. Lynx
H.M.S. Hecla
H.M.S. Tartar
R/V Gillis
R/V Endeavour
N.O. Noroit
R/V Conrad
R/V Malcolm Baldridge
R/V Ronald H. Brown
R/V Ronald H. Brown
R/V Nautilus
R/V Nautilus
R.R.S. James Cook
R.R.S. James Cook
Bathymetry Data
Study Multi−beam Dataset
Data Unavailable − from Lindsay et al. (2005)
Data Unavailable − from Watlington et al. (2002)
T−Phase Events
Visible signs of eruption and T−Phase record
T−Phase record only

Figure 3.

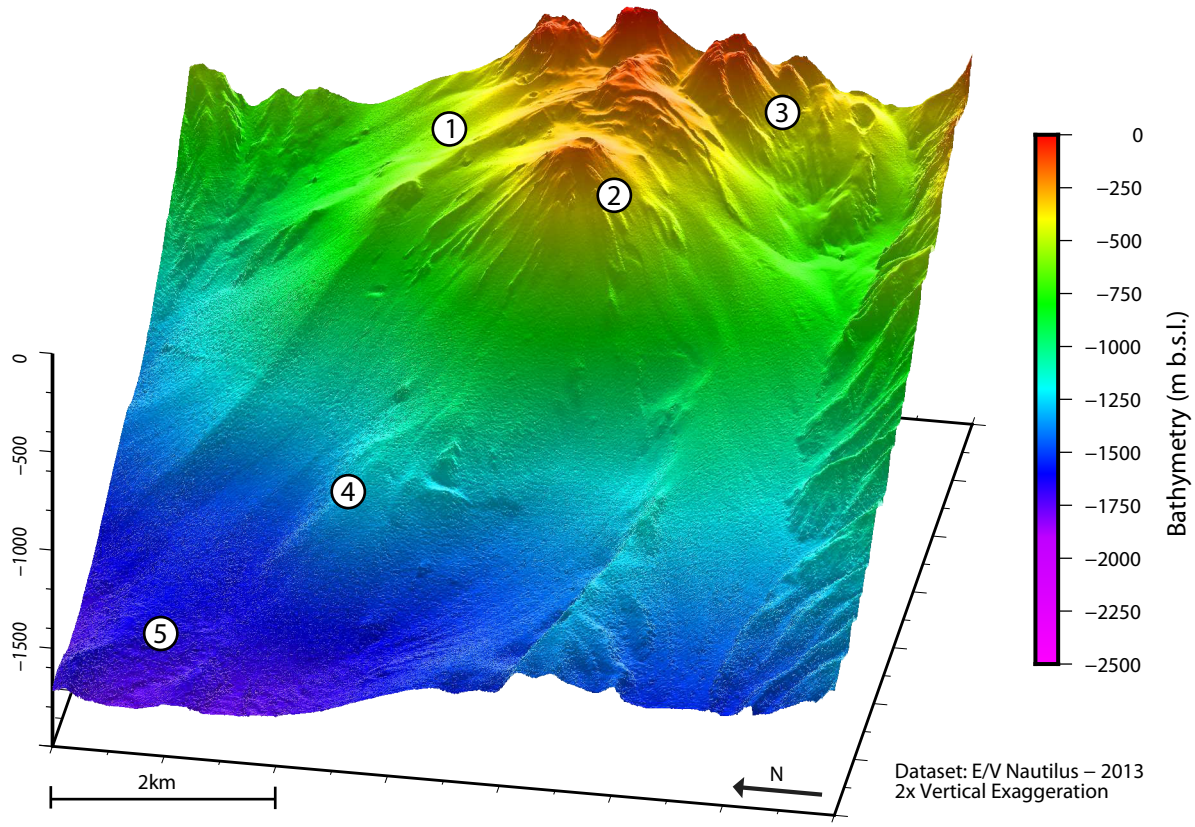
1
2
3
4
5
0
−500
−1000
−1500
2km
N
0
−250
−500
−750
−1000
−1250
−1500
−1750
−2000
−2250
−2500
Bathymetry (m b.s.l.)
Dataset: E/V Nautilus – 2013
2x Vertical Exaggeration

Figure 4.

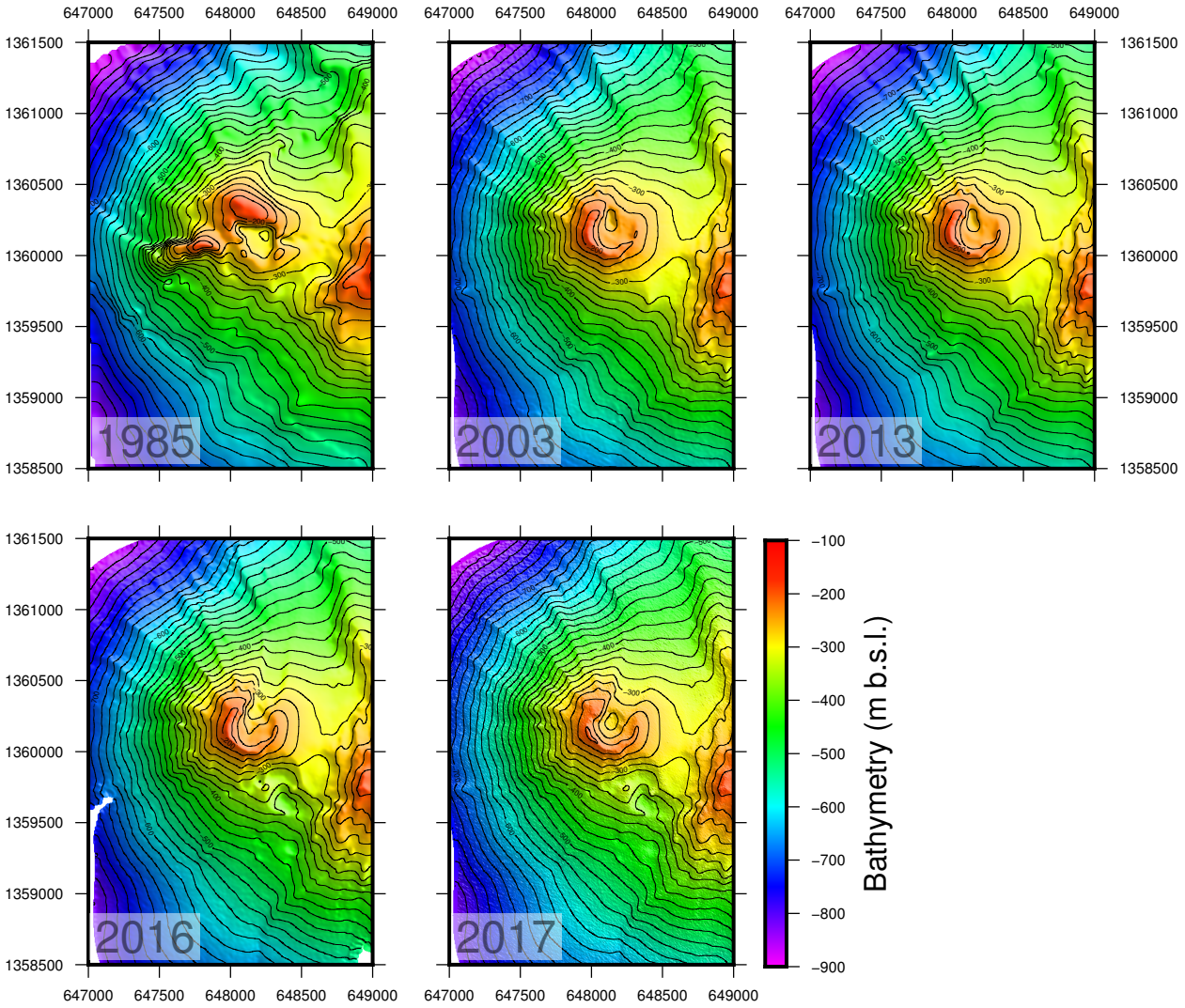
647000
647500
648000
648500
649000
1361500
1361000
1360500
1360000
1359500
1359000
1358500
1985
2003
2013
2016
2017
−100
−200
−300
−400
−500
−600
−700
−800
−900
Bathymetry (m b.s.l.)

Figure 5.

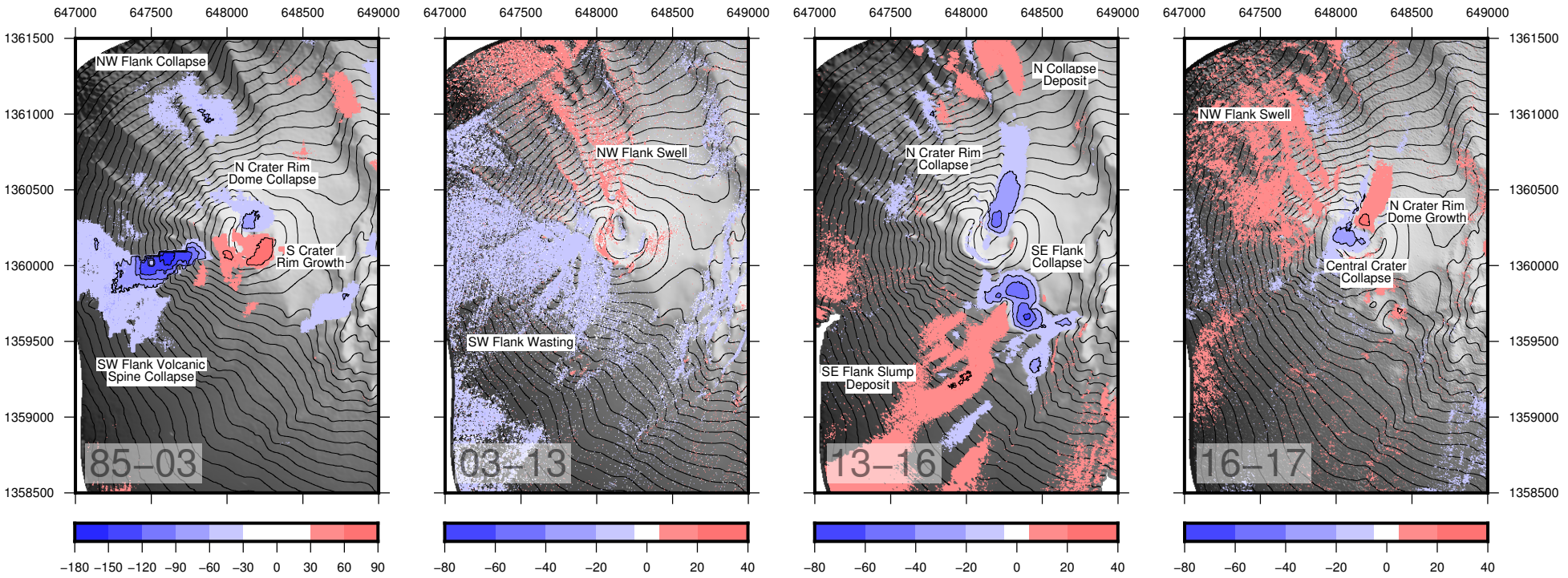
647000
647500
648000
648500
649000
1361500
1361000
1360500
1360000
1359500
1359000
1358500
NW Flank Collapse
N Crater Rim
Dome Collapse
S Crater
Rim Growth
SW Flank Volcanic
Spine Collapse
85–03
−180 −150 −120 −90 −60 −30 0 30 60 90
NW Flank Swell
SW Flank Wasting
03–13
−80 −60 −40 −20 0 20 40
N Collapse
Deposit
N Crater Rim
Collapse
SE Flank
Collapse
SE Flank Slump
Deposit
13–16
−80 −60 −40 −20 0 20 40
NW Flank Swell
N Crater Rim
Dome Growth
Central Crater
Collapse
16–17
−80 −60 −40 −20 0 20 40

Figure 6.

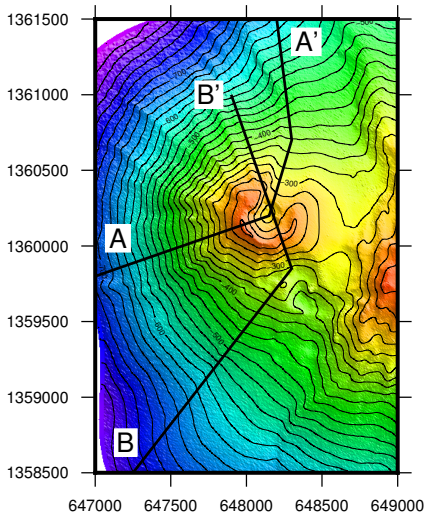

Bathymetry Datasets
- R.R.S. James Cook (2017)
- R.R.S. James Cook (2016)
- E/V Nautilus (2013)
- R.V. Conrad (1985)

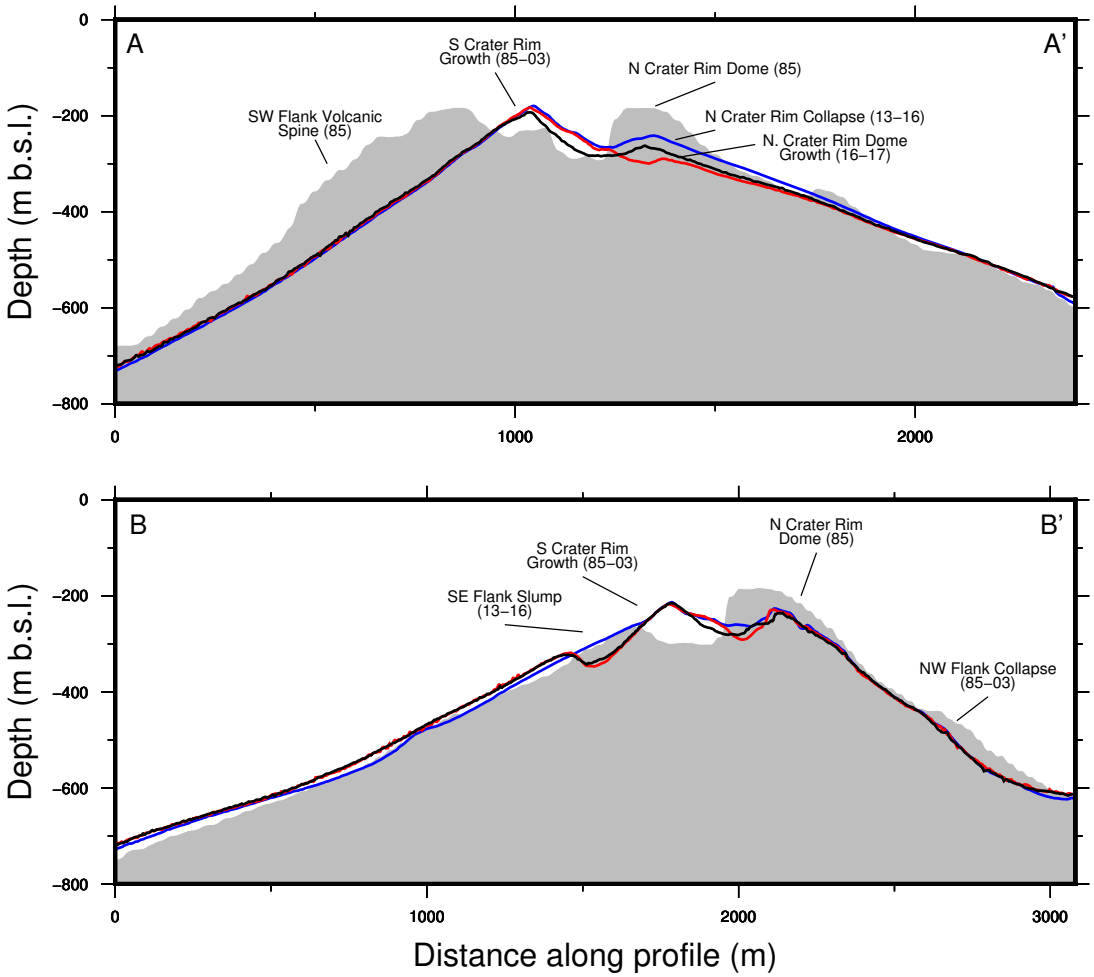

Figure 7.

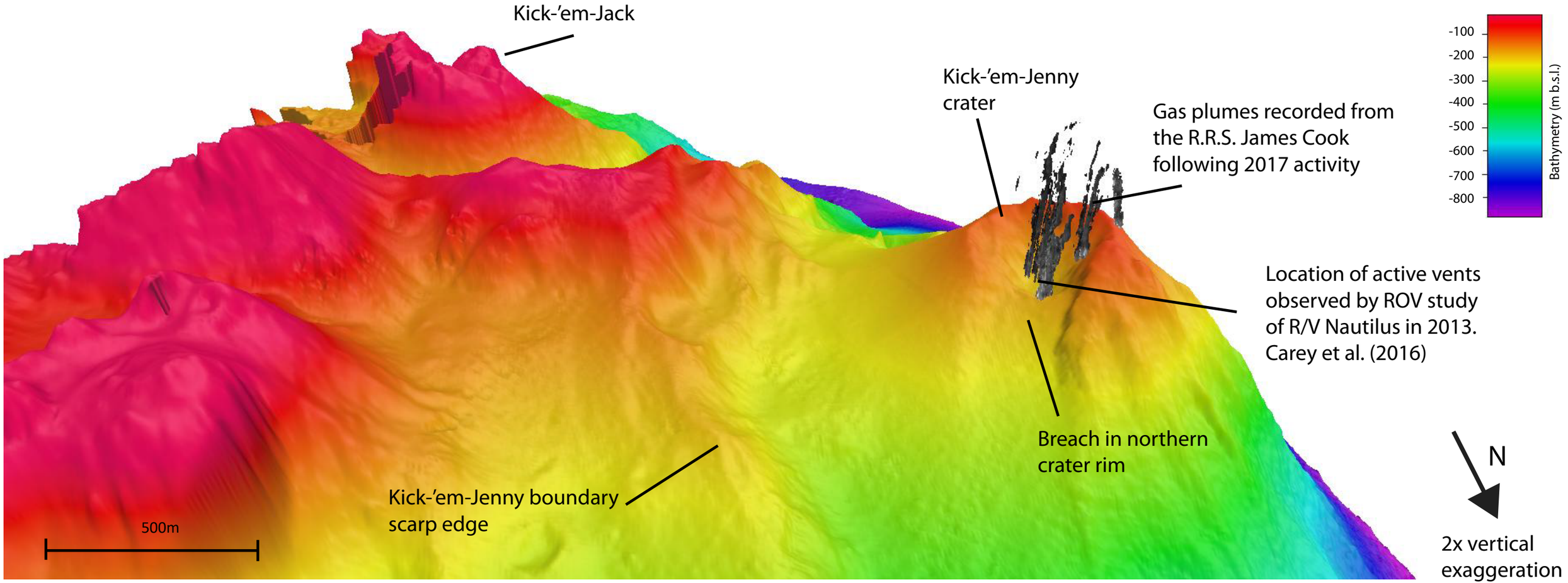
Kick-'em-Jack
Kick-'em-Jenny crater
Gas plumes recorded from the R.R.S. James Cook following 2017 activity
-100
-200
-300
-400
-500
-600
-700
-800
Bathymetry (m b.s.l.)
Location of active vents observed by ROV study of R/V Nautilus in 2013. Carey et al. (2016)
Breach in northern crater rim
Kick-'em-Jenny boundary scarp edge
500m
N
2x vertical exaggeration